Optimum Design of a New 4-DOF Parallel Mechanism

Jae Heon Chung*, Byung-Ju Yi*, and Whee Kuk Kim**

* School of Electrical Engineering and Computer Science, Hanyang University, Ansan, Gyeonggi, Korea
(Tel : +82-31-400-5218; E-mail: bj@hanyang.ac.kr)
**Department of Control and Instrumentation, Korea University, Chochiwon, Korea

Abstract: Recently, lots of parallel mechanisms for spatial 3-DOF and 6-DOF were investigated. However, research on 4-DOF and 5-DOF parallel mechanisms has been very few. In this paper, we propose a 4-DOF parallel mechanism that consists of 3-rotational and 1-translational motions. The kinematic characteristics of this mechanism are analyzed in terms of an isotropic index and maximum force transmission ratio, and its kinematic optimization is being conducted to ensure enhanced kinematic performances

Keywords: Parallel mechanism, Kinematic analysis

1. INTRODUCTION

Recently, lots of parallel mechanisms for spatial 3-DOF and 6-DOF were investigated. However, when an operational space is requested less than 6-DOF or more than 3-DOF, the candidate will be to have 4-DOF and 5-DOF parallel mechanism. Fang and Tsai [4] proposed 4-DOF parallel mechanism with four-link limbs and three-link limbs. Wang and Gosselin [5] analyzed planar a 4-DOF kinematically redundant parallel mechanism and a spatial spherical 4-DOF kinematically redundant structure. Zlantanov and Gosselin [6] proposed parallel architecture with four degrees of freedom that consists of four 5R legs. Huang and Li [7] proposed type synthesis of 4-DOF parallel mechanisms that have three categories. It consists of three rotations + one translation, three translations + one rotation, and two rotations + two translations. Li and Huang [8, 9] analyzed 3-5R parallel mechanism family whose limb consists of a 2R and a 3R parallel subchains or presented a family of symmetrical lower-mobility parallel mechanisms with spherical and parallel sub chains, which consist of two 5-DOF, one 4-DOF and five 3-DOF parallel mechanisms. Company et al. [10] presented a family of fully parallel robots producing motions of the Schoenflies displacements sub-group for high-speed handling and machining. Choi et al. [11] deal with the design and dynamic control simulation of a 4-DOFs parallel mechanism providing 3 translations and 1 rotation for high speed handling and machining. D. chablat and P. Wenger [12] proposed a modular parallel mechanism with 2-translation and 2-rotation motions.

The performance of mechanism can be improved with section of optimized link parameters found by various optimization methods. Lee et al. [1] applied Powell's method to anthropomorphic robot module with redundant actuators. Lee et al.[2] also applied Powell's method by using exterior penalty function to five bar finger mechanism with redundant actuator and applied genetic algorithm to 6-DOF parallel Haptic device [3].

In this paper, firstly, we analyze the mobility of the 4-DOF system using Grübler's mobility formula and describe the new feature of this parallel mechanism. Secondly, we analyze the reverse position of an internal and external chain and obtain the embedded Jacobian by using external Jacobian and internal Jacobian. Thirdly, we describe kinematic design indices (the isotropic index, max force transmission ratio, and workspace). Fourthly, we find optimized link parameters by genetic algorithm to improve the kinematic performance indices. Finally, we show that the performance of the mechanism with the optimized link parameter is superior to the non-optimized mechanism with arbitrary parameters.

2. STRUCTURE

2.1 Mobility

Mobility is defined as the number of independent variables that are required to specify all the motions of the system relative to another. The mobility of the mechanism could be found from well-known Grübler's mobility formula as below:

$$M = D(L-1) - \sum_{i=1}^{j}(D - F_i), \tag{1}$$

where D represents the maximum motion space (6 for spatial motion, 3 for planar motion), and L, F_i, and J represent the number of links including the ground, the number of degree of freedom of the i th joint, and the number of joints, respectively. From Eq. (1), when D=6, L=11 and J=14, the mobility of the mechanism shown in Fig. 1 is 4.

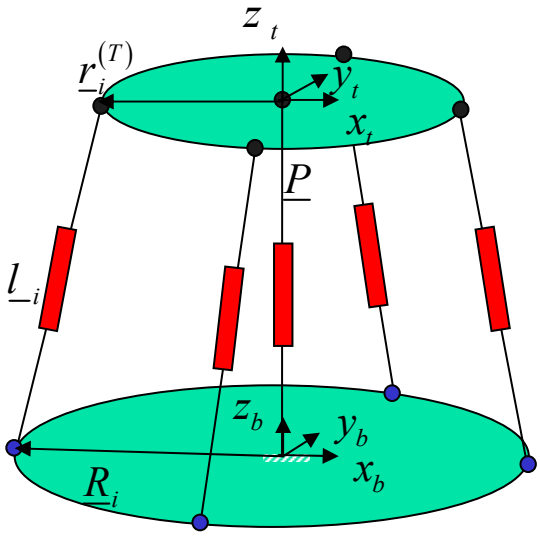

Fig. 1 The description of mechanism

2.2 Description of mechanism

This mechanism consists of four external legs with UPS (universal, prismatic, and spherical) structure, an internal leg with PS (prismatic and spherical) structure, a top plate, and a base plate. The advantage of the system includes a large workspace and high stiffness because of the parallel structure. Specially, this system is constrained by the internal leg not to move in the x- and y- directions. There is no prior 4-DOF mechanism that constrains the x and y motion by this way.

Another merit of this mechanism having an internal leg is that it can support a large payload applied to the horizontal direction. Denote $\underline{P} = [x_t \quad y_t \quad z_t]^T$ as the position vector from the origin of the base frame to the origin of the output frame. So, the position vector of the output can be expressed as $[0 \quad 0 \quad z]^T$ because of the fixed x and y position. $\underline{r}_i$ and $\underline{R}_i$ represent the position vector from the origin of the base plate to the i^{th} universal joint of the external leg and the position vector from the origin of the top plate to the i^{th} spherical joint of external leg, respectively. $\underline{l}_i$ denotes the position vector from the i^{th} universal joint to the i^{th} spherical joint of the external leg.

3. Position analysis

3.1 Reverse position

Reverse position analysis is to find the active input vector when the output position/orientation vector of the mechanism is given. Denote the orientation matrix of the output frame as $[R_b^t]$ using the $x-y-z$ Euler angle set: that is,

$$[R_b^t] = [Rot(\mathbf{x},\alpha)][Rot(\mathbf{y},\beta)][Rot(\mathbf{z},\gamma)] = \begin{bmatrix} c_\beta c_\gamma & -c_\beta s_\gamma & s_\beta \\ s_\alpha s_\beta c_\gamma + c_\alpha s_\gamma & -s_\alpha s_\beta s_\gamma + c_\alpha c_\gamma & -s_\alpha c_\beta \\ -c_\alpha s_\beta c_\gamma + s_\alpha s_\gamma & c_\alpha s_\beta s_\gamma + s_\alpha c_\gamma & c_\alpha c_\beta \end{bmatrix}. \quad (2)$$

The position vector $\underline{P}$ for the ith external leg can be expressed as

$$\underline{P} = \underline{R}_i + \underline{l}_i - \underline{r}_i, \text{ for } i = 1,2,3,4 \quad (3)$$

where

$$\underline{r}_i = [R_b^t]\underline{r}_i^{(T)}. \quad (4)$$

Rewriting Eq. (3) with respect to $\underline{l}_i$ yields

$$\underline{l}_i = \underline{P} + \underline{r}_i - \underline{R}_i. \quad (5)$$

The value of the input variable $\underline{l}_i$ can be found by taking inner product of itself as follows:

$$\underline{l}_i \bullet \underline{l}_i = l_i^2 = (\underline{P} + \underline{r}_i - \underline{R}_i) \bullet (\underline{P} + \underline{r}_i - \underline{R}_i) \quad (6)$$

Reverse position of the internal chain can be directly obtained from the given output position.

3.2 First-order kinematics

To obtain relation between the active input joint vector and an independent output vector in operational space, we start to obtain the first-order kinematics for each of five legs, namely four external legs and an internal leg.

Firstly, the first order kinematics of the external legs can be obtained in the following way. Assume that active joints are located in prismatic joints of the external leg. Therefore, the first-order kinematics of the external legs can be obtained by differentiating Eq.(6) as follows

$$l_i \dot{\underline{l}}_i = \dot{\underline{P}} \bullet (\underline{P} + \underline{r}_i - \underline{R}_i) + \dot{\underline{r}}_i \bullet (\underline{P} + \underline{r}_i - \underline{R}_i), \quad (7)$$

$$l_i \dot{\underline{l}}_i = \underline{l}_i \bullet \dot{\underline{P}} + (\underline{r}_i \times \underline{l}_i) \bullet \underline{\omega}. \quad (8)$$

Eq. (8) can be expressed as the matrix form

$$\begin{bmatrix} l_1 & & & \\ & l_2 & & \\ & & l_3 & \\ & & & l_4 \end{bmatrix} \begin{bmatrix} \dot{l}_1 \\ \dot{l}_2 \\ \dot{l}_3 \\ \dot{l}_4 \end{bmatrix} = \begin{bmatrix} \underline{l}_1^T & (\underline{r}_1 \times \underline{l}_1)^T \\ \underline{l}_2^T & (\underline{r}_2 \times \underline{l}_2)^T \\ \underline{l}_3^T & (\underline{r}_3 \times \underline{l}_3)^T \\ \underline{l}_4^T & (\underline{r}_4 \times \underline{l}_4)^T \end{bmatrix} \begin{bmatrix} \underline{v} \\ \underline{\omega} \end{bmatrix}, \quad (9)$$

where $\underline{v}$ and $\underline{\omega}$ denote a linear velocity vector and an angular velocity vector in the operational space, respectively. The relationship between the active joint and the output velocity vector can be expressed as

$$\dot{\underline{\phi}}_a = [G_u^a]\dot{\underline{u}}, \quad (10)$$

where $\dot{\underline{\phi}}_a$ and $\dot{\underline{u}}$ denote an active joint velocity vector and output velocity vector in operational space, respectively. $[G_u^a]$ can be expressed as

$$[G_u^a] = \begin{bmatrix} l_1 & & & \\ & l_2 & & \\ & & l_3 & \\ & & & l_4 \end{bmatrix}^{-1} \begin{bmatrix} \underline{l}_1^T & (\underline{r}_1 \times \underline{l}_1)^T \\ \underline{l}_2^T & (\underline{r}_2 \times \underline{l}_2)^T \\ \underline{l}_3^T & (\underline{r}_3 \times \underline{l}_3)^T \\ \underline{l}_4^T & (\underline{r}_4 \times \underline{l}_4)^T \end{bmatrix}. \quad (11)$$

Secondly, the first-order kinematics of the internal leg can be obtained as

$$\dot{\underline{u}} = \begin{bmatrix} 0 & 0 & 0 & 0 \\ 0 & 0 & 0 & 0 \\ 1 & 0 & 0 & 0 \\ 0 & 1 & 0 & s_{i3} \\ 0 & 0 & c_{i2} & -s_{i2}c_{i3} \\ 0 & 0 & s_{i2} & c_{i2}c_{i3} \end{bmatrix} \dot{\underline{\phi}}_I = [G_{\phi_I}^u]\dot{\underline{\phi}}_I, \quad (12)$$

where $\dot{\underline{\phi}}_I$ and $[G_{\phi_I}^u]$ denote a joint velocity vector of the internal leg and the relation between the output velocity vector in the operational space and $\dot{\underline{\phi}}_I$, respectively. The output velocity $\dot{\underline{u}}$ of Eq (12) can be separated as the independent and dependent output vectors

$$\dot{\underline{u}} = \begin{bmatrix} \dot{\underline{u}}_p \\ \dot{\underline{u}}_I \end{bmatrix} = [G_{\phi_I}^U]\dot{\underline{\phi}}_I = \begin{bmatrix} [G_{\phi_I}^{u_P}] \\ [G_{\phi_I}^{u_I}] \end{bmatrix} \dot{\underline{\phi}}_I, \quad (13)$$

where $\dot{\underline{u}}_p = [\dot{x} \quad \dot{y}]^T$ and $\dot{\underline{u}}_p = [\dot{z} \quad \omega_x \quad \omega_y \quad \omega_z]^T$ denote a passive output and a active output velocity vector, respectively.

Finally, we embed Eq. (12) into the external Jacobian matrix Eq. (10). An Embedded first-order kinematics can be obtained from relation between independent output vector and the active joint velocity vector by using the constraint relation between the internal leg and the external leg. From Eq. (13), we can derive the relation between the passive output ($\dot{\underline{u}}_P$) and independent output velocity vector ($\dot{\underline{u}}_I$) as the follows

$$\dot{\underline{u}}_p = [G_{\phi_I}^{u_P}][G_{\phi_I}^{u_I}]^{-1}\dot{\underline{u}}_I = [G_{u_I}^{u_P}]\dot{\underline{u}}_I. \quad (14)$$

So, the relations between the output velocity ($\dot{\underline{u}}$) and the independent output velocity vector can be expressed as

$$\dot{\underline{u}} = \begin{bmatrix} \dot{\underline{u}}_I \\ \dot{\underline{u}}_P \end{bmatrix} = \begin{bmatrix} I_{4\times4} \\ [G_{u_I}^{u_P}] \end{bmatrix} \dot{\underline{u}}_I = [G_{u_I}^u]\dot{\underline{u}}_I, \quad (15)$$

where $I_{4\times4}$ denotes an 4 by 4 identity matrix. Substituting Eq. (15) into Eq. (10), we have

$$\dot{\underline{\phi}}_a = [G_{u_I}^a]\dot{\underline{u}}_I, \quad (16)$$

where $[G_{u_I}^a]$ can be expressed as

$$[G_{u_I}^a] = [G_u^a][G_{u_I}^u]. \quad (17)$$

Finally, we can obtain the first-order kinematic relation

$$\dot{\underline{u}}_I = [G_a^{u_I}]\dot{\underline{\phi}}_a. \quad (18)$$

4. KINEMATIC DESIGN INDICES

4.1 Workspace

One of the basic aspects in robot design is to determine the workspace. The operating region or workspace of a manipulator could be defined as a reachable and dexterous workspace, accordingly. The volume of reachable workspace is used in this analysis and defined as

$$V = \int_V dV \ . \tag{19}$$

4.2 Isotropic index

The kinematic Isotropic Index is defined as

$$\sigma_I = \frac{\sigma_{\min}\left(\left[G_a^{u_I}\right]\right)}{\sigma_{\max}\left(\left[G_a^{u_I}\right]\right)}, \tag{20}$$

where $\sigma_{\min}$ and $\sigma_{\max}$ denotes the minimum and the maximum singular value of $\left[G_a^{u_I}\right]$, respectively. When σ_I becomes unity, the end-effector can generate uniform velocity in all directions. In addition, the global design index, which represents the average of the manipulator's isotropic index over the whole workspace, is defined as

$$\Sigma_I = \frac{\int_V \sigma_I dV}{\int_V dV} \ . \tag{21}$$

The greater Σ_I is, the better isotropy the mechanism has over the workspace. Therefore, Σ_I should be maximized.

4.2 Force transmission ratio

The maximum force transmission ratio implies the maximum magnitude of an actuator load required for the unit end-effector force, and it is defined as

$$\sigma_F = \sigma_{\max}\left(\left[G_a^{u_I}\right]\right). \tag{22}$$

IF σ_F becomes smaller, the actuator load will be reduced. This means that the manipulator can bear more weight with less actuator. The global design index for σ_F is defined as

$$\Sigma_F = \frac{\int_V \sigma_F dV}{\int_V dV} \ . \tag{23}$$

The smaller Σ_F is, the smaller capacity actuator required. Thus, Σ_F should be minimized.

5. OPTIMUM DESIGN

In order to maximize the performance of the proposed mechanism, a multi-criteria design methodology based on genetic optimization algorithm is employed

5.1 Composite design index

Several methodologies have been proposed to cope with a multi-criteria based design. However, various design indices are usually incommensurate concepts because of the differences in unit and physical meanings, so should therefore not be combined unless they are transferred into a common domain. This process consists of normalization, which transfers various indices to the same domain, and then combines several indices into one. For both indices V and Σ_I, the most favored preference is given the maximum value, and the least favored preference is given the minimum value of the criterion. Then, the preference design indices, $\tilde{V}$ and $\tilde{\Sigma}_I$ are expressed as

$$\tilde{V} = \frac{V - V_{\min}}{V_{\max} - V_{\min}}, \tag{24}$$

$$\tilde{\Sigma}_{KSI} = \frac{\Sigma_{KSI} - (\Sigma_{KSI})_{\min}}{(\Sigma_{KSI})_{\max} - (\Sigma_{KSI})_{\min}}, \tag{25}$$

where "~" on each design index implies that it is transferred into the common preference design domain. Conversely, for $\tilde{\Sigma}_F$, the highest preference is given the maximum value of the criterion. Then the preference design indices, $\tilde{\Sigma}_F$ is expressed as

$$\tilde{\Sigma}_F = \frac{(\Sigma_F)_{\max} - \Sigma_F}{(\Sigma_F)_{\max} - (\Sigma_F)_{\min}} \ . \tag{26}$$

To deal with this multi-criteria based design, we employ a kinematic composite design index (KCDI) that combines several individual preference design indices into a unique design index by using the max-min principle of fuzzy theory. KCDI is expressed as

$$KCDI = \min\left\{\tilde{V}, \tilde{\Sigma}_{KSI}, \tilde{\Sigma}_F\right\}. \tag{27}$$

KCDI is defined as the minimum value among the preferred design indices calculated for a set of kinematic parameters. A set of design parameters, which have the maximum value of the KCDI, is chosen as the optimal set of design parameters. When any of single design indices, which are included in construction of the KCDI, is weighted more than the others, a weighted KCDI can be used. A weighted KCDI can be represented as

$$KCDI = \min\left\{V^{\alpha}, \tilde{\Sigma}_{KSI}^{\ \beta}, \tilde{\Sigma}_F^{\ \gamma}\right\}, \tag{28}$$

where α, β, and γ represent the weighting for each design index. In this work, all of the weighting is set to 1.0 in order to evenly satisfy the design objectives for all design indices.

5.2 Optimization result

The kinematic design parameters for the proposed mechanism are the radius of the top plate, link length of each leg, and the radius of the base plate. Bounds of these design parameters are described in Table 1.

Genetic algorithm is employed to solve the nonlinear kinematic optimization. We set the population size to 10. In each generation, we evaluate the KCDI of each chromosome, select new population with respect to the probability distribution based on fitness values, and alter the chromosomes in the new population by mutation and crossover operator. After a number of generations, we obtain the best chromosome (i.e., parameter set) that represents an optimal solution. The optimization result is represented in Table 1.

Table 1 optimization result

Variables	Min	Max	Optimization value
Prismatic length [m]	0.1	0.7	0.2971
Top radius [m]	0.1	0.7	0.3379
Base radius [m]	0.3	1.0	0.5821

6. SIMULATION RESULT

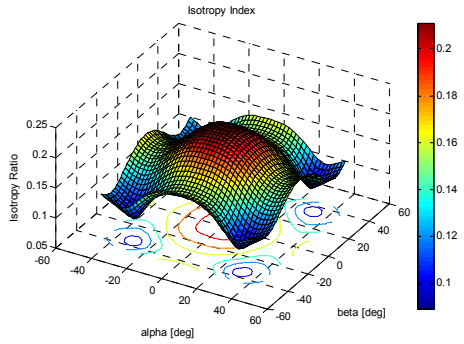

(a) at the z=0.3

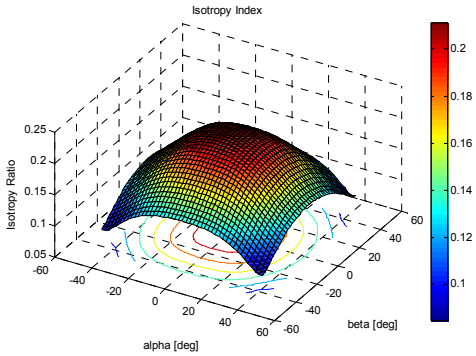

(b) at the z=0.5

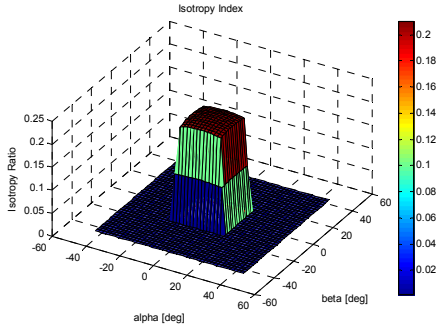

(c) at the z=0.7

Fig.2 Isotropic index before optimization

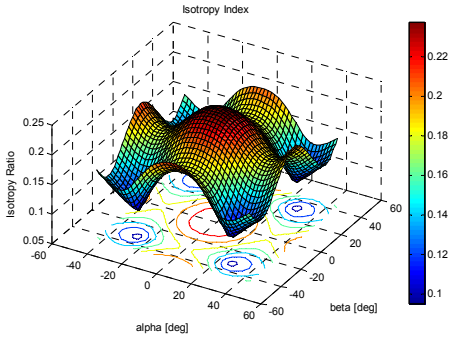

(a) at the z=0.3

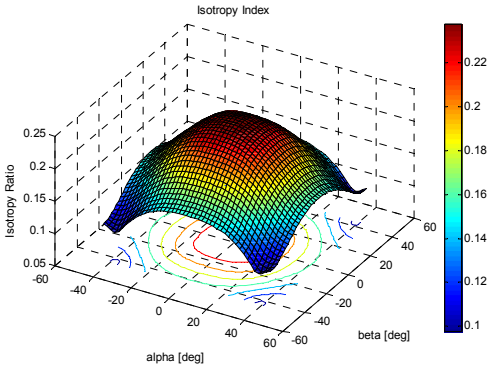

(b) at the z=0.5

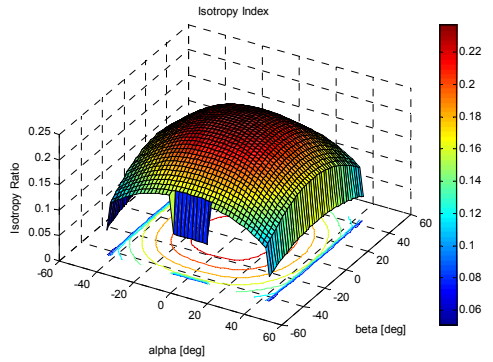

(c) at the z=0.7

Fig. 3 Isotropic index after optimization

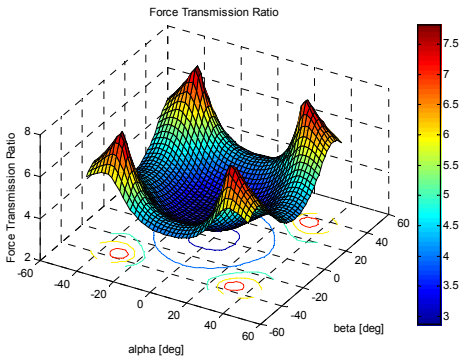

(a) at the z=0.3

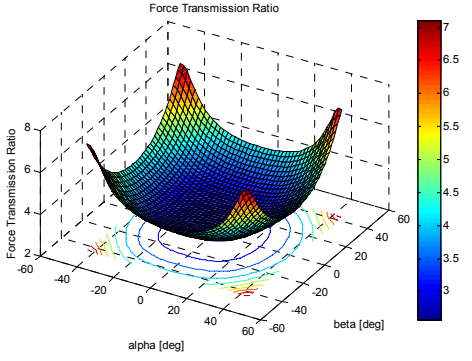

(b) at the z=0.5

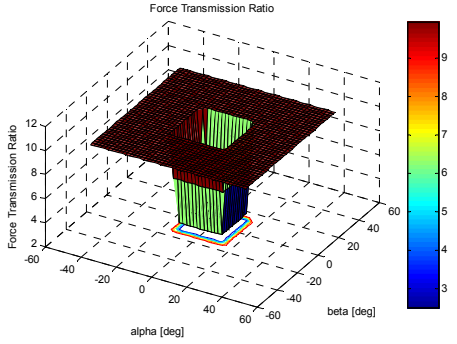

(c) at the z=0.7

Fig.4 Max force transmission ratio before optimization

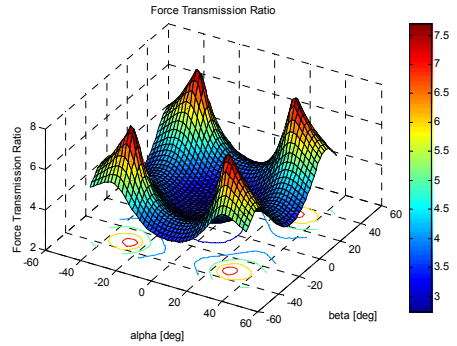

(a) at the z=0.3

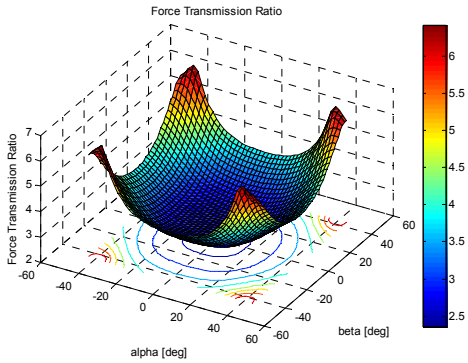

(b) at the z=0.5

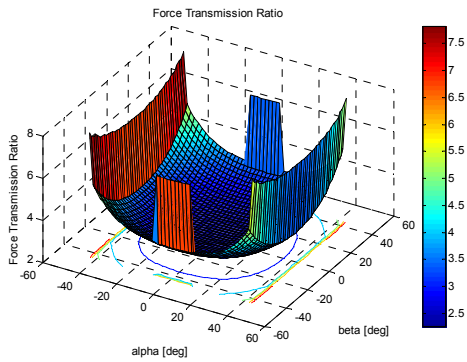

(c) at the z=0.7

Fig. 5 Max force transmission ratio after optimization

Fig. 2 shows the isotropic index before optimization at z =0.3, 0.5, and 0.7. Fig. 3 shows the isotropic index after optimization at z =0.3, 0.5, and 0.7. Fig. 3(c) shows that isotropic performance was improved much compared to Fig. 2 (c). Fig. 4 shows the max force transmission ratio before optimization at z =0.3, 0.5, and 0.7. Fig. 5 shows the max force transmission ratio after optimization at z =0.3, 0.5, and 0.7. Fig. 4(c) shows that force transmission ratio performance was improved much compared to Fig. 5 (c).

Conclusively, we can conclude that the optimized kinematic design parameters improved the kinematic performances of the mechanism significantly.

7. CONCLUSION

We proposed a new 4-DOF parallel mechanism (3-rotation + z-axis translation). We derived Jacobian matrix that relates the active joint to the independent output. We analyzed the performance of this mechanism in aspect of three kinematic indices. Moreover, we find optimal kinematic design parameters of the new mechanism by using genetic algorithm and showed that performances of kinematic indices were improved.

ACKNOWLEDGMENTS

This work was supported by a grant of the Korea Health 21 R&D Project, Ministry of Health & Welfare, Republic of Korea. (02-PJ3-PG6-EV04-0003)

REFERENCES

[1] S. H. Lee, B-J. Yi and Y.K. Kwak, “Optimal Kinematic Design of an Anthropomorphic Robot Module with Redundant Actuators,” *Mechatronics*, Vol. 7, No. 5, pp. 443-464, 1997.

[2] J. H. Lee, B-J. Yi, S-R. Oh and I. H. Suh, “Optimal Design and Development of a Five-bar Finger with Redundant Actuation,” *Mechatronics*, Vol. 11, No. 1, pp. 27-42, 2001.

[3] J. H. Lee, K. S. Eom, B-J. Yi and I. H. Suh, “Design of a New 6-DOF Parallel Haptic Devices,” *Proc. Intl. Conf. on Robotics and Automation*, pp.886-891, 2002.

[4] Y. Fang and L-W. Tsai, “Structure Synthesis of a Class of 4-DOF and 5-DOF Parallel Manipulators with Identical Limb Structures,” *Journal of Robotics Research*, Vol. 21, No. 9, pp. 799-810, 2002.

[5] J. Wang and C. M. Gosselin, “Kinematic Analysis and Design of Kinematically Redundant Parallel Mechanisms,” *Journal of Mechanical Design*, Vol. 126, No. 1, pp.109-118, 2004.

[6] D. Zlantanov and C. M. Gosselin, “A New Parallel Architecture with Four Degree of Freedom,” *Proc. The 2nd workshop on Computational kinematics*, pp.57-66, 2001.

[7] Z. Huang and Q. C. Li, “Type Synthesis of Symmetrical Lower-mobility Parallel Mechanisms Using the Constraint-synthesis Method,” *Journal of robotics research*, Vol. 22, No. 1, pp. 59-79, 2003.

[8] Q. C. Li and Z. Huang, “Mobility Analysis of a Novel 3-5R Parallel Mechanism Family,” *Journal of Mechanical Design*, Vol. 126, No. 1, pp. 79-82, 2004.

[9] Q. C. Li and Z. Huang, “A Family of Symmetrical Lower-Mobility parallel Mechanisms with Spherical and Parallel Subchains,” *Journal of Robotic Systems* Vol. 20, No. 6, pp-297-305, 2003.

[10] O. Company, F. Marquet, and F. Pierrot, “A New High-Speed 4-DOF Parallel Robot Synthesis and Modeling Issues,” *IEEE Trans. on Robotics and Automation*, Vol. 19, No. 3, pp. 411-420, 2003.

[11] H. B. Choi, O. Company, F. Pierrot, A. Konno, T. Shibukawa, and M. Uchiyama, "Design and Control of a Novel 4-DOFs Parallel Robot H4," *Proc. Intl. Conf. on Robotics and Automation*, pp.1183-1190, 2003.

[12] D. Chablat and P. Wenger, "A New Concept of Modular Parallel Mechanism for Machining Applications," *Proc. Intl. Conf. on Robotics and Automation*, pp.3965-3970, 2003.